

Alkyl Coupling on Copper, Silver, and Gold: Correlation between the Coupling Rate and the Metal–Alkyl Bond Strength

Anumita Paul¹ and Brian E. Bent²

Department of Chemistry, Columbia University, New York, New York 10027

Received September 27, 1993; revised December 14, 1993

Recent studies have shown that high coverages of alkyl groups can be generated and isolated on metal surfaces under ultrahigh vacuum conditions by the thermal [Zaera, F., *Acc. Chem. Res.* 25, 260 (1992)] and photochemical [Zhou, X.-L., Zhu, X.-Y., and White, J. M., *Surf. Sci. Rep.* 13, 74 (1991)] dissociation of alkyl halides. This paper describes studies in which these approaches have been employed to study the coupling of methyl groups generated on a Au(111) surface. The coupling rate, as measured by temperature-programmed reaction experiments, is found to be sensitive to the structure of the surface. For a well-annealed surface, coupling occurs at ~270 K, but for a sputtered and incompletely annealed surface, coupling occurs at ~350 K. An interesting and unexpected finding is that coadsorbing P(CH₃)₃ with the methyl groups on a Au(100) surface inhibits the coupling reaction so that methyl radical desorption is observed. Similarities between the rates of methyl coupling and methyl radical desorption have also been observed previously for a Cu(111) surface, suggesting a correlation between the methyl coupling rate and the metal–alkyl bond strength. Such a correlation can account for the trends in the coupling rates reported for alkyl groups on Ag(111), Au(100), Cu(111), and Cu(110). The coupling rate is fastest on surfaces and for alkyl groups that are expected to form the weakest carbon–metal bonds. © 1994 Academic Press, Inc.

1. INTRODUCTION

The coupling of alkyl fragments on metal surfaces to form carbon–carbon bonds is conceptually simple but poorly understood. Intuitively, one expects factors such as reaction thermodynamics, the rate of diffusion across the surface, and steric bulk of the alkyl to play a role, but each of these factors is difficult to quantify experimentally. The situation is particularly challenging, since alkyl groups readily dehydrogenate on most metal surfaces, especially under ultrahigh vacuum (UHV) conditions under which the surface coverage of hydrogen is low.

The exceptions in this regard are the coinage metals: copper, silver, and gold. These metals are known for their inability to dehydrogenate hydrocarbons, making them potential candidates for studying the coupling of adsorbed alkyls.

A recent series of elegant studies by Zhou, White, and co-workers has shown that Ag(111) surfaces couple adsorbed alkyls under UHV conditions to liberate alkanes (1–9). As summarized in Table 1, a variety of alkyls as well as vinyl (CH₂CH) and phenyl (C₆H₅) groups were generated on Ag(111) by thermal, photochemical, or electron-impact dissociation of alkyl halides. In each case, alkyl coupling is the primary reaction pathway on the surface, and no dehydrogenation is observed. The role of the coadsorbed halogen in the coupling reaction was studied by comparing the chemistry of vinyl and phenyl groups formed by (a) thermal dissociation of the corresponding iodide (CH₂CHI or C₆H₅I) and (b) electron-induced dissociation of the corresponding hydrocarbon (ethylene or benzene). The effect of the halogen on coupling of these unsaturated hydrocarbon fragments is to lower the coupling activation energy by several kcal/mol (9).


A significant finding from the studies of Zhou and White is that the coupling rate depends strongly on the identity of the alkyl group, as evidenced by the wide range of temperature-programmed reaction (TPR) peak temperatures for these processes (see Table 1). Ethyl and isopropyl groups couple below 200 K, while phenyl groups do not couple until 375 K. This temperature difference corresponds to a difference in rate of about six orders of magnitude at 300 K.

Interestingly, the substantially different alkyl coupling rates on Ag(111) do not correlate with steric bulk as one might expect. Sterically unhindered methyl groups, for example, couple at a temperature ~60 K higher than both ethyl and isopropyl groups. The coupling rates are also counter to the C–C bond energies in the coupled product. Hydrocarbon fragments which couple to form the strongest C–C bonds have the highest coupling temperature, i.e., the slowest coupling rate (see Table 1). Since these

¹ Present address: Department of Chemical Engineering, Carnegie Mellon University, Pittsburgh, PA 15213.

² Presidential Young Investigator, A. P. Sloan Fellow, and Camille and Henry Dreyfus Teacher–Scholar.

TABLE 1
Alkyl Coupling on Ag(111)^a

Alkyl precursor	Coupling ^b temperature (K)	Activation ^c energy (kcal/mol)	Bond energy ^d (kcal/mol)	
			C-I	C-C
C ₂ H ₅ I	175–220	10.0 ± 2.0	54	82
<i>i</i> -C ₃ H ₇ I	184–192	10.5–11.5	54	79
<i>n</i> -C ₃ H ₇ I	203–211	11.5–13.0	54	82
CH ₃ I	250–260	15.0–16.0	56	88
CH ₂ =CHI	250–260	15.2 ± 1.5	61 ^e	110
 -I	380–390	26.2 ± 2.0	66	116

^a Numerical values from Refs. (8, 9).

^b Temperature-programmed reaction (TPR) peak temperatures; the heating rates were 2.5–4 K/s. In each case, the TPR peak temperature is determined by the rate of the coupling reaction.

^c Assuming pseudo-first-order preexponential factors of 10¹³ s⁻¹.

^d From R. T. Sanderson, "Chemical Bonds and Bond Energy," 2nd ed. Academic Press, New York, 1976.

^e Estimated based on the C-Cl bond energy and trends in carbon halogen bond energies for other molecules.

coupling reactions are probably exothermic by 10–40 kcal/mol (10), this result is consistent with the Hammond postulate which predicts a reactant-like, as opposed to a product-like, transition state for exothermic reactions (13). One might, therefore, expect that the coupling rates on metal surfaces would reflect the metal-carbon bond strengths (11), with weaker metal-carbon bonds giving rise to faster coupling rates. Such a comparison is difficult to make, since metal-carbon bond strengths are not generally known. However, if we assume that metal-carbon bond strengths show a trend similar to those for carbon bonding to other atoms, then the trends in the C-C and C-I bond energies given in Table 1 suggest that the hydrocarbon fragments which form the strongest metal-carbon bonds have the slowest coupling rates.

In this paper, we present results for methyl coupling on Au(111) and Au(100) surfaces and summarize recent results for methyl coupling on copper surfaces which provide direct evidence for a correlation between the metal-alkyl bond strength and the alkyl coupling rate. Specifically, it is shown that methyl coupling to form ethane and methyl radical desorption from the surface occur at comparable rates on Au(100) and on Cu(111). The dependence of the alkyl coupling rate on the nature of the metal (copper vs silver vs gold), the structure of the surface (Au(100) vs Au(111)), and the structure of the alkyl group (methyl vs longer chain alkyls) is also discussed, and a comparison with theoretical predictions is presented.

2. EXPERIMENTAL

The experiments were performed in two UHV systems which have been previously described in Refs. (12, 14). The Au(111) and Au(100) surfaces were purchased as oriented and polished wafers from the Cornell Dept. of Materials Science and from Monocrystals Ltd., respectively. The Au(111) surface was mounted using Ta tabs to hold the crystal in contact with a resistive heating element (12). The Au(100) surface was tied to a resistive heating element by wrapping a wire around the grooved edge of the crystal (14). In both cases, the surface temperature was measured by a chromel-alumel thermocouple junction which was wedged into a 0.05-mm-diameter, 2–3-mm-deep hole at the side of the crystal and the samples could be cooled to ~100 K by contact with a liquid-nitrogen-cooled copper block. The precision of the thermocouple readings from the two crystals was evaluated based on the multilayer desorption peak temperatures for C₂H₅I on both surfaces. In both cases, the peak temperature for a 7-L exposure (~1.5 layers) was 130 K.

The gold surfaces were cleaned by sputtering and annealing as previously described (15). Iodomethane (CH₃I, Aldrich) was adsorbed by backfilling the chambers, and exposures are reported in Langmuirs (L) where 1 L = 10⁻⁶ Torr · s. Trimethylphosphine (P(CH₃)₃), which was used to inhibit the methyl coupling reaction so that methyl radical desorption could be detected, was obtained from Professor G. Parkin, and its purity was verified *in situ* by mass spectrometry. P(CH₃)₃ was adsorbed using a pin-hole doser to avoid large background pressures of this extremely "sticky" molecule. Exposures are reported in seconds; for reference, a 110-s exposure is required to saturate the monolayer at 100 K. Methylgold trimethylphosphine, CH₃AuP(CH₃)₃, which was adsorbed to generate an equimolar mixture of CH₃ and P(CH₃)₃ on the Au(100) surface, was obtained from IBM (16) and was sublimed (vapor pressure at room temperature ~ 10⁻⁴ Torr) onto the surface from a differentially pumped and collimated source. The mass spectrum of the dosing gas and the details of the source are presented elsewhere (17). For reference, a 180-s exposure saturates the monolayer (17).

In the temperature-programmed reaction experiments, the adsorbate-covered surfaces were held 1–2 mm from 2-mm-diameter apertures to differentially pumped mass spectrometers and heated at 3 K/s. For the photodissociation experiments, a 1000-W high pressure mercury arc lamp was used to produce photons with wavelengths down to 230 nm. The source was apertured and focused through a quartz window into the UHV chamber. The focused beam was ~1 cm in diameter (slightly larger than the diameter of the Au(111) crystal), and the power at the surface, as determined from a mock-up of the experimen-

tal geometry outside the UHV chamber, was 70 mJ/cm² at 250–575 nm.

3. RESULTS AND INTERPRETATION

Here, we present the results for methyl coupling on Au(111) and Au(100) surfaces and the results for methyl radical evolution from Au(100). In Section 4, these results are compared with results in the literature to address the following issues: correlation between the metal–alkyl bond energy and the alkyl coupling rate, effects of molecular structure and surface structure on the coupling rate, and differences between the methyl coupling rates on the (111) faces of copper, silver, and gold.

3.1. Methyl Coupling on Au(111)

Methyl groups were generated on a Au(111) surface by the thermal and photochemical dissociation of CH₃I. For a clean and 900-K-annealed Au(111) surface, there is no detectable thermal dissociation of CH₃I. All the CH₃I desorbs molecularly intact. However, if the surface is annealed to only 800 K after sputtering, a small amount of dissociative adsorption is observed. This dissociative adsorption, which presumably occurs at defect sites, is evidenced by *m/e* = 27 and 30 evolution 350 K in the temperature-programmed reaction (TPR) spectra shown in Fig. 1A. The *m/e* 27 : 30 ratio of 1.3 for these peaks is consistent with ethane formation due to methyl coupling. The photodissociation experiments described below establish that it is the coupling of adsorbed methyl groups which gives rise to this product. Furthermore, on the basis of the finding that molecular CH₃I desorbs from Au(100) at temperatures below 280 K, we rule out the possibility that carbon–iodine bond dissociation is the rate-determining step in ethane formation at 350 K.

Adsorbed CH₃ was generated at 110 K on a Au(111) surface by photodissociating submonolayer coverages of CH₃I. Typical results are shown in Fig. 1B. In this experiment, a well-annealed Au(111) surface precovered with 1 L of CH₃I at 110 K was exposed to 1.8×10^{13} photons/cm² (total exposure time = 360 sec). The photodissociation of adsorbed CH₃I on silver surfaces to produce adsorbed methyl groups has been well documented (5–7). On Au(111), the adsorbed methyl groups, formed by the photodissociation reaction at 110 K, couple to evolve ethane at 270 K as shown by the *m/e* = 27 and 30 TPR curves in Fig. 1B. Consistent with CH₃I photodissociation and formation of ethane, the molecular desorption yield decreases after exposing the surface to UV light, as shown by the molecular desorption spectra for CH₃I in the bottom of Fig. 1B. Using the calibration of our mass spec-

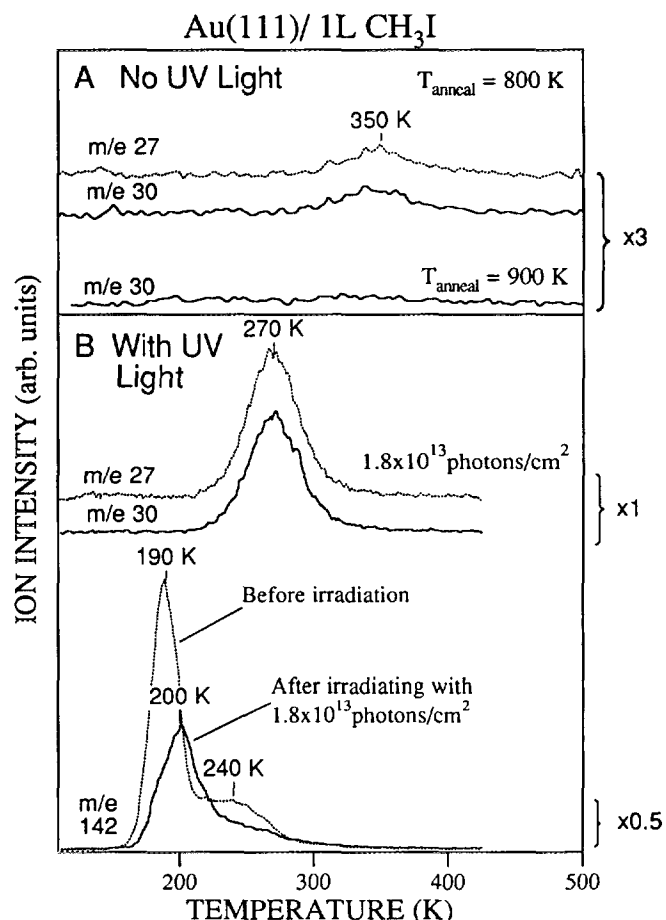


FIG. 1. Formation and coupling of CH₃ groups on Au(111). (A) Temperature-programmed reaction (TPR) spectra of the indicated ions after a 1-L exposure of CH₃I at 110 K. The differences in the two traces for *m/e* = 30 are attributed to the presence of surface defects as a result of annealing the Au(111) surface to 800 vs 900 K after sputtering. (B) TPR spectra of the indicated ions after exposing a Au(111) surface to 1 L of CH₃I at 110 K followed by irradiation with 1.8×10^{13} photons of UV light. The decrease in the molecular desorption yield upon irradiation and the concurrent increase in the evolution of ethane (as monitored here by *m/e* = 27 and 30) are attributed to formation and coupling of adsorbed methyl groups.

trometer for ethane and CH₃I (see Ref. (15)) and the experimentally measured 67% decrease in the molecular desorption yield, we calculate that the fraction of CH₃I groups photodissociated on the surface is 14%, and the fraction which photodesorb is 53% for a 6-min exposure to UV radiation.

Note that the methyl coupling temperature on the smooth Au(111) surface is 80 K below that for coupling on the rough surface (see Fig. 1). This difference suggests that methyl groups bind more strongly to defect sites than to the (111) terraces. This result does not imply, however, that coupling necessarily occurs at defect sites on the

rough surface. The coupling reaction on the rough surface could still occur on the (111) terraces but have a slower rate simply because the equilibrium between the terraces and defects favors bonding at the defect sites.

3.2. Methyl Coupling on Au(100)

Unlike the results on Au(111), some CH_3I thermally dissociates even on a well-annealed Au(100) surface. Methyl groups generated on the surface by this dissociation reaction couple to produce ethane with a TPR peak temperature which shifts from 375 to 330 K with increasing coverage. The peak shape and peak temperature shift are characteristic of second order reaction kinetics, consistent with methyl coupling being the rate-determining step in ethane evolution. Detailed studies of this reaction are presented in Ref. 17. For the purposes of this discussion, the important point to note is that the coupling temperature is significantly above 270 K, that of methyl coupling on Au(111). This difference is not attributable to inaccuracies in the thermocouple readings which are on the order of ± 10 K (see Section 2).

The Au(100) and Au(111) coupling results along with those reported elsewhere (15, 18) for longer chain alkyl groups on these surfaces are summarized in Table 2. These results are discussed further in Section 4.

TABLE 2
Alkyl Coupling on Gold Surfaces

Alkyl precursor	Coupling temperature (K) ^a [Activation energy (kcal/mol)] ^b	
	Au(111)	Au(100)
CH_3I	270 ^c [16.5]	330–375 ^d [20.4–22.5]
$\text{C}_2\text{H}_5\text{I}$	260–270 ^e [15.9–16.5]	260–320 ^f [15.9–19.7]
$n\text{-C}_3\text{H}_7\text{I}$	260–270 ^e [15.9–16.5]	—
$n\text{-C}_4\text{H}_9\text{I}$	260–270 ^e [15.9–16.5]	—

^a Temperature-programmed reaction peak temperatures; heating rates were 3 K/s.

^b Assuming a pseudo-first-order preexponential factor of 10^{13} s^{-1} .

^c This work; the coupling temperature on a sputtered and incompletely annealed surface is 350 K.

^d Reference (17); temperature range reflects the coverage dependence.

^e Reference (15); temperature range reflects the coverage dependence.

^f Reference (18); minor amounts of competing disproportionation products are evolved concurrently.

3.3. Methyl Radical Desorption from Au(100) and Cu(111)

An unexpected finding during studies of the reactions of CH_3 on Au(100) was that trimethylphosphine ($\text{P}(\text{CH}_3)_3$) inhibits methyl coupling so that methyl radical desorption can be observed. This effect is shown in Fig. 2A. At the top of Fig. 2A are TPR spectra for $m/e = 30$ and $m/e = 15$ after exposing a Au(100) surface to 2.0 L of CH_3I at 250 K. The $m/e = 30$ spectrum corresponds to ethane evolution, while the $m/e = 15$ peak corresponds to molecular desorption of CH_3I which was adsorbed during cooling of the surface after the exposure. By exposing this same monolayer to sufficient $\text{P}(\text{CH}_3)_3$ to saturate the surface, ethane evolution is completely suppressed, as shown by the TPR spectrum for $m/e = 30$ in the bottom of Fig. 2A. In its place, $m/e = 15$ is detected evolving from the surface at 415 K. TPR spectra at $m/e = 142$ show that the $m/e = 15$ evolution is not due to molecular CH_3I desorption. The $m/e = 15$ peak is due to methyl radicals, as established by the results presented below.

The assignment of the $m/e = 15$ peak in Fig. 2A to methyl radicals was hampered by the concurrent detection of $m/e = 16$ due to CH_4 formation from CH_3 reaction with the chamber walls. This effect is shown in Fig. 2B for the adsorption of $\text{CH}_3\text{AuP}(\text{CH}_3)_3$ which generates an equimolar mixture of CH_3 and $\text{P}(\text{CH}_3)_3$ on the surface (17). While the $m/e = 15$ and 16 peaks have the same shape and peak temperature, suggesting a single product, the 16:15 ratio of 0.33 is far from that of 1.22 for methane. The mass spectrometer signal at $m/e = 15$ from methane and methyl radicals was distinguished by investigating the $m/e = 15$ intensity as a function of the electron impact ionization energy, and the results are shown in the inset. The open symbols show the $m/e = 15$ signal evolved during the experiment at the bottom of Fig. 2B as a function of the ionizer energy, while the closed symbols are the $m/e = 15$ intensity for a methane standard leaked into the chamber. Both data sets have been normalized to the same value for an ionizer energy of 80 eV. The important conclusion from these results is that the threshold for CH_3^+ ($m/e = 15$) formation from the surface reaction product is ~ 5 eV below that for methane. This is the same difference reported in the literature for $m/e = 15$ formation from methane and methyl radicals (19). This observation, combined with the fact that no higher mass peaks besides $m/e = 16$ are detected, leads us to conclude that the surface reaction product is methyl radicals and that the methane formed is due to methyl radical reaction with the chamber walls.

Methane interference in the mass spectrometric detection of methyl radicals has been noted in a number of previous studies of methyl radical evolution from surfaces

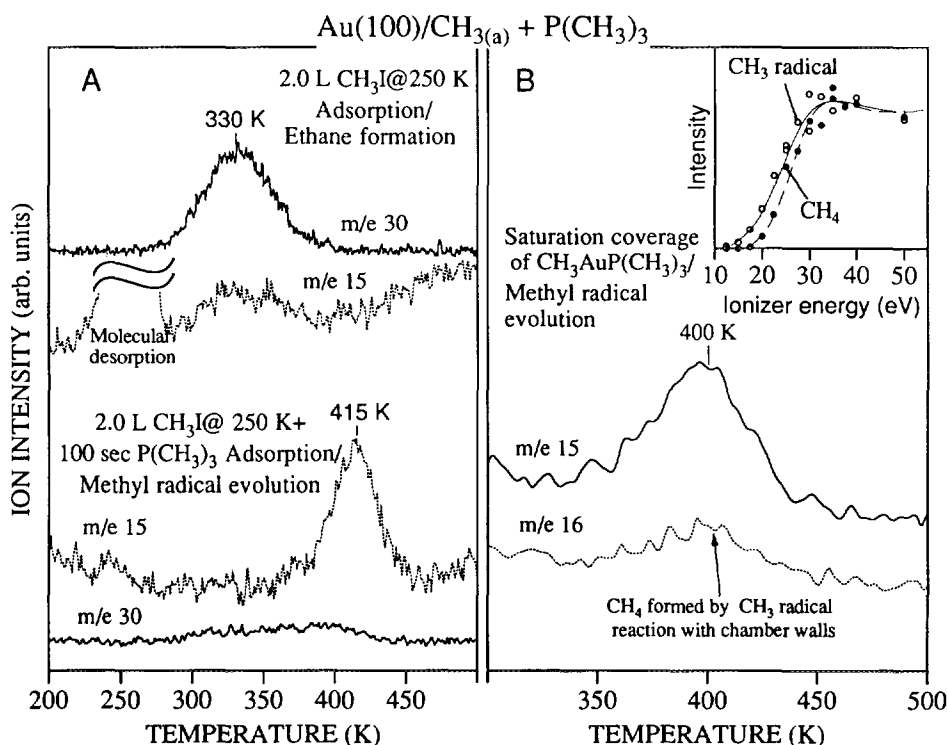


FIG. 2. Effects of P(CH₃)₃ coadsorption on the reaction of CH₃ groups on a Au(100) surface. (A) Comparison of the $m/e = 30$ (ethane) and $m/e = 15$ (methyl radical) evolution with and without coadsorbed P(CH₃)₃ after a 2 L CH₃I exposure at 250 K to generate adsorbed CH₃ groups. (B) Temperature-programmed reaction spectra for $m/e = 15$ and 16 after adsorbing a monolayer of CH₃AuP(CH₃)₃ on Au(100) to generate a stoichiometric ratio of CH₃ and P(CH₃)₃ on the surface. The inset compares the dependence of the $m/e = 15$ TPR signal on the electron impact ionization energy with the intensity of the $m/e = 15$ fragment for a methane standard.

(20–22). Most relevant for the results here are studies of methyl radical evolution from Cu(111) during the thermal decomposition of CH₃I (22). These studies were performed in the same apparatus as the results reported here, and the $m/e = 16:15$ ratio of 0.30 matches that of 0.33 in these studies to within the experimental uncertainty. Furthermore, in studies with CD₃I on Cu(111), CD₃⁺ ($m/e = 18$) and CD₃H⁺ ($m/e = 19$) but not CD₄⁺ ($m/e = 20$) were detected. The presence of CD₃H and the absence of CD₄ is strong evidence that the methane comes from a reaction with the chamber walls and not with the Cu(111) surface. It should be noted that even though the methane molecular ion at $m/e = 16$ is ~30% of the $m/e = 15$ peak for methyl radicals, the methane formed is only about 7% of the methyl radical yield since the mass spectrometer sensitivity is higher for methane by a factor of 4.4. This calibration is discussed in Ref. (23).

The significance of methyl radical evolution is that the reaction activation energy provides a direct measure of the metal–methyl bond energy (given the reasonable assumption that there is no barrier for CH₃ adsorption on the surface). In the case of methyl radical evolution from Au(100), the studies in which CH₃I is coadsorbed with

P(CH₃)₃ or in which CH₃AuP(CH₃)₃ is adsorbed on the surface show a CH₃ radical TPR peak temperature of 400–415 K. Deriving kinetic parameters from TPR spectra is not straightforward, but if we assume a standard value of 10¹³ sec⁻¹ for the preexponential factor for desorption, the peak temperature for CH₃ desorption from Au(100) corresponds to an activation energy of 25 kcal/mol. If we also make the reasonable assumption that there is no barrier for methyl adsorption on Au(100), then this activation energy is equal to the gold–carbon bond energy. In the case of CH₃ evolution from Cu(111), the peak temperature of 470 K corresponds to an activation energy for desorption of ~29 kcal/mol. These values are accurate to ± 2 kcal/mol for an uncertainty of ± 100 in the assumed value for the preexponential factor.

An important consideration in these radical evolution results is the potential effect of the coadsorbed species (P(CH₃)₃ on Au(100) and iodine on Cu(111)) on the metal–carbon bond energy. The fact that in both cases the coadsorbed species are required in order to observe CH₃ radical desorption suggests that the coadsorbed species promote radical desorption by weakening the metal–carbon bond. On the other hand, the radical evolu-

tion temperature in both systems shows essentially no shift with variation in the coadsorbate coverage (17, 23). Instead, it appears that the effect of coadsorbed iodine on Cu(111) is to block surface sites where the CH_3 groups decompose (23) and that the main effect of $\text{P}(\text{CH}_3)_3$ on Au(100) is to inhibit CH_3 coupling through an ensemble effect (17). In other words, the results suggest that coadsorbates are required to observe CH_3 desorption from Au(100) and Cu(111) primarily because they inhibit competing CH_3 reactions as opposed to promoting CH_3 desorption.

4. DISCUSSION

4.1. Correlation Between the Metal-Alkyl Bond Energy and the Alkyl Coupling Rate

The results here and in the literature for methyl coupling on copper, silver, and gold are summarized in Fig. 3, which plots the temperature ranges of the TPR peaks observed for this reaction. Also shown are the temperature ranges for methyl radical evolution from Au(100) and Cu(111). It is interesting that not only does the radical peak temperature on Cu(111) correlate with the higher coupling temperature on this surface, but also that coupling and radical desorption occur at nearly the same temperatures for the two surfaces on which both of the reactions have been observed. While the similarity between the temperatures for methyl coupling and methyl desorption in these two systems may be fortuitous, the results indicate that the stronger metal-carbon bond has

the slower (higher temperature) coupling reaction. The results therefore provide direct evidence for the hypothesis advanced in the introduction that the alkyl coupling rate correlates with the metal-carbon bond energy. This conclusion is valid whether alkyl diffusion or coupling is the actual rate-determining step in the reaction. It is worth noting that the metal-carbon bond strength need not necessarily have been correlated with the coupling rate. One can imagine polar transition states for which the energy relative to the reactants' ground state does not correlate with the metal-carbon bond energies.

It should also be noted that the similarity of the methyl coupling and desorption rates does not imply that the methyl coupling pathway proceeds via a radical mechanism. Formation of ethane by reaction of a methyl radical with an adsorbed methyl group would be consistent with the kinetic results, but to our knowledge, there is no precedence for radical attack at such a sterically hindered metal-carbon bond. Radical reactions in such a system would typically result in H abstraction to form methane. The formation of ethane by coupling of two methyl radicals would have an activation energy equal to twice the metal-methyl bond energy and is therefore inconsistent with the experimental results. Further study is needed to determine what factors determine the branching between methyl coupling and methyl desorption.

4.2. Effects of Molecular Structure and Surface Structure on the Alkyl Coupling Rate

The results in Tables 1 and 2 and in Fig. 3 show that the structure of both the alkyl group and the metal surface have significant effects on the alkyl coupling rate. Furthermore, the effects are at least partly consistent with the expected trends in the metal-carbon bond strengths. As noted in the introduction, alkyl groups that would be expected to have stronger metal-carbon bonds have slower coupling rates. For example, on Ag(111) and Au(100), ethyl coupling to form butane occurs at a lower temperature than methyl coupling to form methane. While a direct comparison of metal-methyl and metal-ethyl bond strengths has yet to be made, weaker metal-ethyl bonds are to be expected based on a comparison of the bond strengths of methyl and ethyl to other atoms (see, for example, the C-I bond strengths in Table 1). Similarly, the substantially higher temperature for methyl coupling on Au(100) vs Au(111) (~350 K vs 270 K) may reflect a stronger Au-C bond on the more open (100) surface (24). The similar temperatures for methyl coupling on Cu(111) and Cu(110) are not readily interpreted because the position of the TPD peak is affected by the presence of competing methyl decomposition reactions on these surfaces (12).

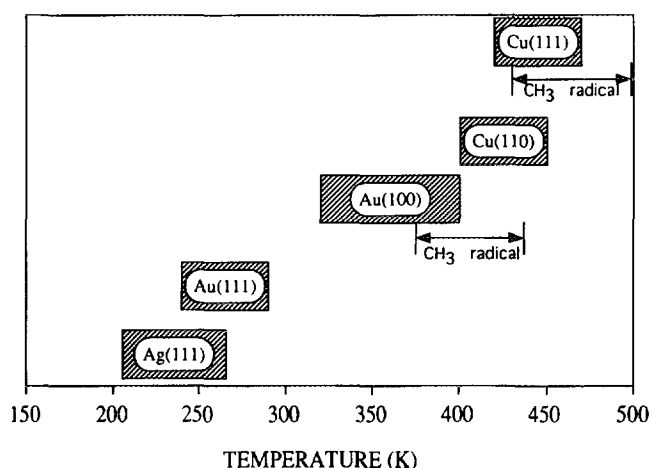


FIG. 3. Temperature ranges for the temperature-programmed reaction peaks for methyl coupling to form ethane on the indicated surfaces of copper, silver, and gold. Also shown are the temperature ranges over which methyl radicals have been detected in TPR experiments of methyl groups coadsorbed with iodine and with $\text{P}(\text{CH}_3)_3$ on Cu(111) and Au(100), respectively.

4.3. Comparison of the Methyl Coupling Rates on Copper, Silver, and Gold

The coupling temperatures summarized in Fig. 3 show that the methyl coupling rate on the (111) surfaces of the coinage metals follows the order silver > gold > copper. The fact that gold lies between copper and silver in this series but lies below them in the periodic table is not surprising. In many of its properties, including cohesive energy (25), melting point (26), and heat of atomization (27), gold is intermediate between copper and silver.

The relative rates of methyl coupling on Cu(111), Ag(111), and Au(111) suggest that the metal-carbon bond strengths follow the order Cu-C > Au-C > Ag-C. However, as noted above, correlations between the metal-carbon strength and the alkyl coupling rate are true regardless of whether it is diffusion across the surface or the coupling reaction itself which is the rate-determining step. On the other hand, calculations at the extended Hückel level by Zheng, Apeloig, and Hoffmann (28) have indicated that if the coupling step, and not diffusion, is rate determining, then the coupling rate should correlate with the position of the metal-carbon bonding orbital relative to the Fermi level of the metal. Provided the energy of the metal-carbon bonding orbital is approximately invariant with metal, the methyl coupling rates on Cu(111), Ag(111), and

Au(111) are consistent with this theoretical prediction. This correlation is illustrated in Fig. 4. As shown, the methyl-metal bonding orbital is initially doubly occupied and the methyl group can be viewed as CH_3^- due to charge transfer from the metal (28). As the methyl groups approach each other, the potential energy of the system initially increases as the C-C bonding and antibonding orbitals, both doubly occupied, begin to form (28). The potential energy continues to increase until the C-C antibonding orbital rises above the Fermi level. At this point, the antibonding electrons can transfer into the metal, and further C-C bond formation is attractive (28). Since the calculated Fermi levels (29) for the coinage metals increase on going from silver to gold to copper, as shown in Fig. 4, this theoretical picture predicts that the coupling rate should follow the trend observed experimentally.

5. CONCLUSIONS

The results here show that methyl groups generated on Au(111) and Au(100) surfaces undergo coupling reactions to produce ethane, and that the coupling rate is significantly faster on the (111) surface than on the (100) surface. In addition, by using $\text{P}(\text{CH}_3)_3$ coadsorption to inhibit the methyl coupling rate on Au(100), methyl radical desorption was observed. The similarity between the activation energies for methyl coupling and methyl radical desorption on Au(100) is analogous to results observed previously for Cu(111), and provides direct evidence for a correlation between the metal-methyl bond strength and the coupling rate. Based on a comparison of the gold results here with those in the literature for copper and silver surfaces, the alkyl coupling rate is shown to be a strong function of the alkyl structure, the surface structure, and the nature of the metal. The dependence of the coupling rate on these parameters correlates with the expected trends in the metal-carbon bond strengths.

ACKNOWLEDGMENTS

We thank the National Science Foundation (CHE-90-22077 and DMR-89-57236) and the Donors of the Petroleum Research Fund, administered by the American Chemical Society, for supporting various aspects of this research.

REFERENCES

1. Zhou, X.-L., Solymosi, F., Blass, P. M., Cannon, K. C., and White, J. M., *Surf. Sci.* **219**, 294 (1989).
2. Zhou, X.-L., and White, J. M., *Catal. Lett.* **2**, 375 (1989).
3. Zhou, X.-L., and White, J. M., *J. Chem. Phys.* **92**, 5612 (1990).
4. Zhou, X.-L., Castro, M. E., and White, J. M., *Surf. Sci.* **238**, 215 (1990).
5. Zhou, X.-L., and White, J. M., *Surf. Sci.* **241**, 244 (1991).
6. Zhou, X.-L., and White, J. M., *Surf. Sci.* **241**, 259 (1991).

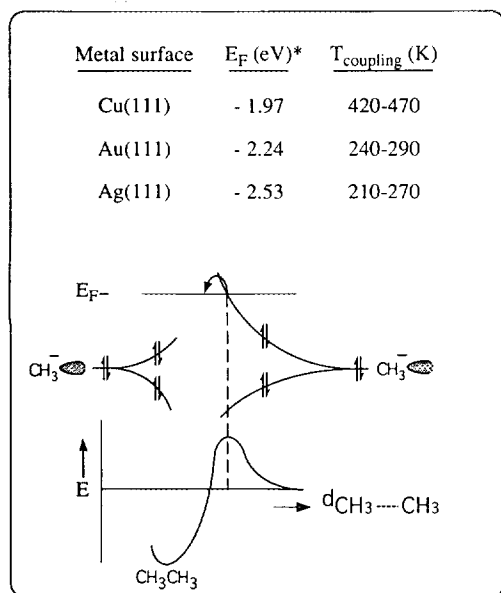


FIG. 4. Schematic diagram based on the theoretical description given by Zheng *et al.* (28) for methyl coupling on metal surfaces. The activation barrier for coupling is correlated with the point at which the antibonding orbital in the incipient C-C bond rises above the Fermi level of the metal so that the methyl groups, which are formally CH_3^- , can transfer an electron back to the metal surface; (*) indicates Fermi level calculation for bulk metal relative to the inner potential (29).

7. Zhou, X.-L., and White, J. M., *Surf. Sci.* **241**, 270 (1991).
8. Zhou, X.-L., and White, J. M., *J. Phys. Chem.* **95**, 5575 (1991).
9. Zhou, X.-L., Schwaner, A. L., and White, J. M., *J. Am. Chem. Soc.* **115**, 4309 (1993).
10. This prediction is based on metal-alkyl bond energies of 25–40 kcal/mol, which is the range typical for metal-alkyl bond energies in molecular compounds (11). Methyl coupling on Cu(110) has been determined to be exothermic by 28 ± 10 kcal/mol (12).
11. Halpern, J., in "Bonding Energetics in Organometallic Compounds" (T. J. Marks, Ed.). ACS Symposium Series, Vol. 428, American Chemical Society, Washington, 1990.
12. Chiang, C.-M., Wentzlaff, T. H., and Bent, B. E., *J. Phys. Chem.* **96**, 1836 (1992).
13. See for example: Harris, J. M., and Wamser, C. C., "Fundamentals of Organic Reaction Mechanisms," p. 124. Wiley, New York, 1976.
14. Lin, J.-L., and Bent, B. E., *J. Phys. Chem.* **96**, 8529 (1992).
15. Paul, A., Yang, M. X., and Bent, B. E., *Surf. Sci.* **297**, 327 (1993).
16. Banaszak Holl, M. M., Seidler, P. F., Kowalczyk, S. P., and McFeely, F. R., *Appl. Phys. Lett.* **62**, 1475 (1993).
17. Paul, A., Bent, B. E., and Seidler, P. F., submitted.
18. Yang, M. X., Jo, S. K., Paul, A., Ávila, L., Bent, B. E., and Nishikida, K., submitted.
19. Levin, R. D. and Lias, S. G., "Ionization Potential and Appearance Potential Measurements." NSRDS-NBS71, 1971–1981. While the absolute values of 9.8 and 14.4 eV reported for the thresholds of $m/e = 15$ formation from CH_3 and CH_4 , respectively, differ by ~5 eV from those shown in the inset of Fig. 2B, the difference is attributable to the uncertainty in the absolute calibration of our mass spectrometer.
20. Serafin, J. G., and Friend, C. M., *J. Am. Chem. Soc.* **111**, 8967 (1989).
21. Creighton, J. R., *Surf. Sci.* **234**, 287 (1990).
22. Lin, J.-L., and Bent, B. E., *J. Am. Chem. Soc.* **115**, 2849 (1993).
23. Lin, J.-L., and Bent, B. E., *J. Phys. Chem.* **97**, 9713 (1993).
24. The effects of surface reconstruction, which occurs on both Au(111) and Au(100), have not been investigated.
25. Kittel, C., "Introduction to Solid State Physics." Wiley, New York, 1976.
26. Emsley, J., "The Elements." Clarendon Press, 1989.
27. "CRC Handbook of Chemistry and Physics," 71st ed. CRC Pr. Boca Raton, 1990–1991.
28. Zheng, C., Apeloig, Y., and Hoffmann, R., *J. Am. Chem. Soc.* **110**, 749 (1988).
29. Andersen, O. K., Jepsen, O., and Glötzel, D., in "Highlights of Condensed Matter Theory," F. Bassani, F. Fumi, and M. P. Tosi, Eds., Proceedings of the International School of Physics Enrico Fermi, Course LXXXIX, Elsevier, Italy, 1985. The calculated values for the Fermi level are used as opposed to work function measurements to avoid surface dipole contributions.
30. Yang, M. X., Paul, A., and Bent, B. E., in preparation.